

Effects of focal injection of kainic acid into the mouse hippocampus *in vitro* and *ex vivo*

Caroline Le Duigou¹, Lucia Wittner¹, Lydia Danglot² and Richard Miles¹

¹INSERM U739, CHU Pitié-Salpêtrière, UPMC, 105 boulevard de l'Hôpital, Paris 75013, France

²INSERM U497, Ecole Normale Supérieure, 46 rue d'Ulm, Paris 75005, France

Intra-hippocampal kainate injection induces an epileptiform activity termed status epilepticus. We examined the emergence of this activity with extracellular and intracellular records of responses (1) to focal kainate (KA) application in slices of mouse hippocampus and (2) of slices from mice injected with KA. The effects varied with distance from the injection site of KA. At distances less than $\sim 800 \mu\text{m}$, KA injection induced a strong increase in extracellular firing which ceased after 2–4 min. Pyramidal cells in this zone fired and depolarized to a potential at which action potentials were no longer evoked. No further activity was detected near the injection site for 3–5 h. In longitudinal slices of the CA3 region, firing induced by KA injection spread at a velocity close to $1 \times 10^{-4} \text{ mm ms}^{-1}$. The velocity increased to $\sim 1 \times 10^{-1} \text{ mm ms}^{-1}$ when synaptic inhibition was blocked, suggesting that inhibitory processes normally restrict the spread of firing. At distances of 1.5–2.5 mm, KA injection induced a short-term increase in firing which was maintained, and often increased and rhythmic at gamma frequencies at 2–5 h after injection. We also examined slices prepared from animals injected with KA, at a delay of 2–5 h corresponding to the expression of status epilepticus. Near the injection site, Gallyas silver staining revealed cellular degeneration, and no activity was recorded. Interictal-like activity was generated by ipsilateral slices distant from KA injection. Contralateral slices also generated an interictal-like activity, but no cell death was detected. Hippocampal oscillations generated at distant sites may be associated with status epilepticus.

(Received 27 July 2005; accepted after revision 18 October 2005; first published online 20 October 2005)

Corresponding author R. Miles: INSERM U739, CHU Pitié-Salpêtrière, 105 boulevard de l'Hôpital, 75013 Paris, France.
Email: rmiles@chups.jussieu.fr

In chronic models of epilepsy, a stimulus induces changes that result in an epileptic brain after a delay of weeks or months. Such stimuli include agonists at glutamate receptors (Ben-Ari *et al.* 1979; Zaczek & Coyle, 1982), kindling (Goddard, 1967), hyperthermia (Baram *et al.* 1997) and ischaemia and hypoxia (Jensen *et al.* 1991). The glutamate agonist kainate (KA) has been especially well studied. KA injection *in vivo* induces a maintained, pathological synchrony termed status epilepticus, which lasts for up to 24 h (Ben-Ari, 1985; Ben-Ari & Cossart, 2000). During this period, a sclerotic death of principal cells (Sater & Nadler, 1988) and specific types of interneurons (Magloczky & Freund, 1993; Bouilleret *et al.* 1999) is initiated. The status epilepticus and cell death have been linked to the delayed emergence of an epileptic network. Typically, recurrent epileptic seizures emerge after several weeks. Long-term reactive changes in cell excitability (Vreugdenhil *et al.* 1998; Chen *et al.* 2001; Misonou *et al.* 2004), synaptic function (Nusser *et al.* 1988; Suzuki *et al.* 2000; Cossart *et al.* 2001) and connectivity (Ribak *et al.* 1979; Sutula *et al.* 1988) may all

contribute to the generation of pathologically synchronous discharges.

In this study we examined events intervening between the application of KA and the emergence of status epilepticus. We made focal intrahippocampal applications of KA in order to distinguish between its local and distant effects (Magloczky & Freund, 1993; Riban *et al.* 2002). KA was injected in acutely prepared slices to investigate immediate events. Slices prepared from animals injected in the same way were also studied to examine the emergence of status epilepticus. Intracellular, multi-unit and field responses were recorded close to and distant from the site of KA injection, to discriminate between the contributions of these different sites to status epilepticus. We found that KA injection caused a strong but transient increase in multi-unit firing near the injection site, and that no further activity was detected at this site. The firing initiated by KA spread slowly through slices. At distant sites, a maintained and often rhythmic activity persisted for several hours after injection. We conclude that the behavioural manifestations of status

epilepticus may depend in part on persistent population activities generated at hippocampal sites distant from the injection.

Methods

Experiments were performed on adult C57BL/6J male mice (Janvier, Le Genest Saint Isle, France), weighing 30–35 g, housed in a 12 h light–dark controlled cycle. All experiments were performed in accordance with the European Committee Council Directive (86/89/EEC) and with INSERM guidelines.

Intrahippocampal kainate acid injection

Adult male mice were anaesthetized with 4% chloral hydrate (120 ml kg⁻¹; Sigma France) and 4% urethane (1000 ml kg⁻¹; Sigma, France), and placed in a stereotaxic frame. Injections were made through a stainless steel cannula of outside tip diameter 0.28 mm, connected to a 0.5 μ l microsyringe (Hamilton, Fisher Labosi, France). A volume of 50 nl kainic acid (Sigma, France) dissolved at 20 mM in 0.9% NaCl was injected into the right dorsal hippocampus (Bouilleret *et al.* 1999). The electrode was maintained in place for 5 min to limit reflux along the injection track. Control animals were prepared identically and injected with the same volume of NaCl. Injections were made at stereotaxic coordinates of Bregma: anteroposterior (AP) = -1.8 mm, mediolateral (ML) = -1.8 mm, dorsoventral (DV) = -1.8 mm. This corresponds to a site in the dorsal hippocampus in the apical dendritic zones of the CA1 region near the hippocampal fissure. Animals typically recovered from anaesthesia after 2–5 h. On recovery they displayed behavioural signs of status epilepticus, including stereotyped turning movements and immobile states.

In experiments to examine the effects of kainic acid in tissue from injected animals, slices were prepared at 1.5–2.5 h after injection, before the animals recovered from anaesthetic. Recordings began at 3–4 h after kainic acid injection. In these experiments the injection solution contained both 20 mM kainic acid and the fluorescent tracer microruby (10 mg ml⁻¹, 3000 Da, Invitrogen, Cergy Pontoise), so that the site of injection could be identified.

In some experiments we examined the extent of diffusion of 50 μ l Rhodamine dextran (10 kDa, lysine fixable, Invitrogen, Cergy Pontoise, France) injected *in vivo* using the same system. Animals were anaesthetized, injected, and after 3 h perfused with 4% paraformaldehyde in 0.1 M phosphate buffer (PB). Brains were removed, cryoprotected overnight in 30% sucrose in PB. Serial sections of thickness 60 μ m were cut at -25°C and permeabilized in a PB solution containing 0.1% Triton and 0.1% gelatin. Neuronal Nissl substance was stained with A488-Neurotrace (Invitrogen). Fluorescence images were acquired with a Leica confocal microscope TCSP2.

Neurotrace was detected using the 488 nm line of an argon laser for excitation, and Rhodamine dextran excited by the 543 nm line of a green neon laser. Typically, 40 confocal sections (1024 \times 1024 pixels) were scanned per tissue section of thickness 60 μ m. Examination of ~20 representative tissue sections from ~80 sections cut around the injection site was sufficient to include all tissue that contained Rhodamine dextran. 3D rendering (Fig. 7D) was done on stacks of ~800 images using the programme Amira (TGS, Mercury Computer Systems, Merignac, France).

Slice preparation and kainic acid injection *in vitro*

Slices were prepared from mice after KA injection, or from uninjected animals. In both cases an intracardiac perfusion was made under chloral hydrate/urethane anaesthesia, with a cold (2–5°C) artificial cerebrospinal fluid (ACSF) containing (mM): 26 NaHCO₃, 1 KCl, 9 MgCl₂, 1 CaCl₂, 248 sucrose and 10 D-glucose. After decapitation, the brain was removed. Hippocampal–cortical slices (Walther *et al.* 1986) or longitudinal CA3 slices (Miles *et al.* 1988) of thickness 400 μ m were cut with a vibratome (Vibratome, St Louis, MO, USA) and placed in an interface recording chamber. They were perfused at 3–4 ml min⁻¹ with an oxygenated (95% O₂/5% CO₂) ACSF containing (mM): 124 NaCl, 4.5 KCl, 1 NaH₂PO₄, 26 NaHCO₃, 2 CaCl₂, 2 MgCl₂, 10 glucose (pH ~ 7.4, 295–310 mosmol l⁻¹) at 35°C, while their upper surface was exposed to a humidified 95% O₂/5% CO₂ atmosphere.

Procedures for KA injection into slices were similar to those used in injecting animals. The same volume and concentration, 50 nl of 20 mM KA in ACSF, or 50 nl of a saline solution of 0.9% NaCl was injected from an identical cannula system with a Hamilton syringe. The cannula was advanced until it just entered the slice before injection. Injections were made at similar apical dendritic sites of the CA1 region in hippocampal–cortical slices, and at apical dendritic sites in longitudinal slices of the CA3 region.

Recording methods and data analysis

Recordings were made during a period of 1–6 h after KA or saline injection. Intracellular recordings from hippocampal and cortical neurones were made using glass microelectrodes filled with 2 M potassium acetate, and bevelled to a final resistance of 50–100 M Ω . Membrane potentials were measured using an Axoclamp 2B amplifier (Axon Instruments, Union City, CA, USA). Multi-unit activity and field potentials were recorded with extracellular electrodes made from tungsten wire of 50 μ m diameter (Phymep, Paris, France). Up to four electrodes were mounted on holders controlled by separate manipulators. Differences in potential between each tungsten electrode and a reference Ag–AgCl electrode were measured using a 4-channel amplifier (AM Systems, model

1700, Carlsborg, WA, USA). Extracellular signals were amplified 1000 × and filtered with pass band between 1 Hz and 10 KHz. Signals were digitized at 10–20 kHz, with a voltage resolution of 0.6 μV for extracellular signals and 25 μV for intracellular signals, using a 12-bit, 16-channel analog-to-digital converter (Digidata 1200 A, Axon Instruments), and visualized on a PC using the programme Axoscope (Axon Instruments).

Action potential frequency was measured from multi-unit records using routines written in the Labview environment (National Instruments Austin, TX, USA). Spikes were detected using an 'up-only' algorithm, and a user-defined threshold (Cohen & Miles, 2000). The programmes are available at <http://glab.bcm.tmc.edu>. Power spectra were constructed from extracellular records, filtered to pass frequencies lower than 100 Hz, using the Clampfit programme (Clampfit 9, Axon Instruments). A Fourier transform was applied to records of duration 2–5 min, using a rectangular window, 50% overlap and a sample number of 32768 which corresponds to a spectral resolution of 0.3 Hz.

Morphology

Cell death was studied using the Gallyas silver impregnation technique (Gallyas *et al.* 1980). Animals were killed at 3 h after the injection of kainate or physiological saline. They were perfused intracardially with cold ACSF, followed by 100 ml of fixative containing 4% paraformaldehyde and 15% saturated picric acid dissolved in 0.1 M phosphate buffer (PB). The brains were then removed, 100 μm-thick sections were cut with a Vibratome and washed in PB. The Gallyas staining procedure consists of a pretreatment with alkaline hydroxylamine, washing in acetic acid, impregnation in silver nitrate in the presence of ferric ions, washing in citric acid, development, and a second wash in acetic acid. It reveals a black silver precipitate which accumulates in the cytoplasm of degenerating cells, while healthy cells are coloured orange. After impregnation, sections were washed in PB, mounted on gelatine-coated slides and covered with DePeX (Laboratoire d.b.h., France).

Distinct populations of interneurons were examined by immunostaining against parvalbumin (PV), calbindin (CB), calretinin (CR) and somatostatin (SOM). Animals were fixed as before with paraformaldehyde and picric acid. The hippocampus and nearby cortex was dissected and sections of thickness 60 μm were cut with a vibratome. Endogenous peroxidase activity was blocked by 1% H₂O₂, and non-specific staining suppressed by 5% milk powder and 2% bovine serum albumin containing 0.1% Triton-X. Monoclonal mouse antibodies against PV (dilution 1:3000, Sigma), CB and CR (1:3000 each, Swant, Bellinzona, Switzerland), and rat polyclonal antibody against SOM (1:200, Chemicon International, Temecula,

USA) were applied with 0.1% Triton-X100 for 24 h at 4°C. Immunostained elements were visualized using biotinylated antimouse and antirat immunoglobulin G (1:250, Vector Laboratories, Burlingame, CA, USA) as the secondary antiserum followed by avidin-biotinylated horseradish peroxidase complex (ABC; 1:250, Vector). The immunoperoxidase reaction was developed by 3,3'-diaminobenzidine tetrahydrochloride (DAB; Sigma), as a chromogen. Sections were osmicated (0.25% OsO₄ in PB, 30 min), dehydrated in ethanol, and mounted in Durcupan (ACM, Fluka).

Results

Immediate actions of kainic acid injection in hippocampal-cortical slices

Kainic acid (KA) injection into hippocampal slices caused an increase in neuronal activity. Subsequent effects differed at sites close to and distant from the injection. While the separation is rather artificial, we will refer to local actions as those induced within ~800 μm of the injection site and those at sites beyond ~1200 μm as distant.

KA was injected at apical dendritic sites of the CA1 region in hippocampal-cortical slices ($n = 23$). Records from sites near the injection in the CA1 and CA3 regions as well as in the dentate gyrus and the subiculum (Fig. 1A E1 and E2) revealed an increase in firing with latency 150–2000 ms. Action potential frequency in multi-unit records increased from values of 68.3 ± 82.7 Hz. (Fig. 1B) to 449.1 ± 203.5 Hz. The increase in firing was accompanied by field potential oscillations at frequencies of 30–100 Hz (Fig. 1C, E1 and E2). Sometimes two waves of increased activity were recorded by electrodes situated in CA3 (15 of 23 slices) and in the subiculum (7 of 23 slices). In all records from sites close to KA injection, spontaneous multi-unit activity ceased completely at 2.5 ± 3.0 min ($n = 46$ CA3 and subicular records), and did not recover (Fig. 1D, E1 and E2).

In the entorhinal cortex at a distance of 2–3 mm from the injection, KA sometimes initiated (in 11 of 23 slices) a smaller increase in multi-unit firing, which occurred with a delay. Firing frequency increased from 3.5 ± 4.5 to 58 ± 44 Hz with a latency of 4.6 ± 4.2 min, and was associated with the appearance of isolated non-rhythmic field potentials (Fig. 1A, E3). In contrast to records from sites close to KA injection, firing in the entorhinal cortex did not cease (Fig. 1D, E3).

Immediate actions of kainic acid injection in longitudinal slices of the CA3 region

We wished to examine the spread of firing induced by KA injection, and to compare local and distant effects in a similar structure. Experiments were therefore repeated in

longitudinal slices of length 3–4 mm prepared from the CA3 region (Fig. 2).

KA injection induced a rapid increase in local firing in longitudinal CA3 slices ($n = 24$ of 26 slices; Fig. 2A, E1). The frequency of detected multi-unit firing increased from 3–60 Hz to 50–600 Hz, and was associated with field potential oscillations at frequencies of 30–100 Hz (Fig. 2B, E1; Fig 2D, E3). Near the injection site (Fig. 2C and D, E1), spontaneous discharges ceased at 37.1 ± 26.6 s after injection (mean \pm s.d., $n = 26$).

Records from multiple sites, revealed a unidirectional spread of activity induced by KA (Fig. 2A). The mean propagation speed, measured to the onset of the increase in firing, was $9 \times 10^{-5} \pm 6 \times 10^{-5}$ mm ms⁻¹ (Fig. 2E). This velocity is slower than that of conduction in non-myelinated hippocampal axons (~ 0.2 mm ms⁻¹; Raastad & Shepherd, 2003), and might indicate that activity spreads by the diffusion of kainate (Nicholson, 2001). At the site of injection, activity ceased in most slices (22 of 26) at 8.34 ± 6.77 min after KA injection. In contrast, activity was maintained at sites more distant than ~ 1 mm. In 15 records from distant sites in 26 slices, the frequency of firing remained increased after 15 min.

KA-induced firing spread slowly throughout longitudinal slices. We compared this spread to that of epileptiform discharges induced by disinhibition (Miles *et al.* 1988). In the presence of bicuculline

($20 \mu\text{M}$; $n = 5$), a spontaneous interictal-like activity propagated throughout the CA3 region (Fig. 3A). Its velocity, measured from differences in latencies of events recorded with three extracellular electrodes, was 0.12 ± 0.08 mm ms⁻¹ ($n = 5$). We then injected KA into disinhibited slices. It induced a local increase of activity, which spread at a speed of 0.11 ± 0.07 mm ms⁻¹ (mean \pm s.d., $n = 5$) much more rapidly than in the absence of bicuculline (Fig. 3A). These data suggest that synaptic inhibition normally prevents the rapid spread of KA-induced firing. In the presence of synaptic inhibition, the spread seems to be mediated by mechanisms other than axonal or polysynaptic transmission.

One possible mechanism is that KA diffuses through the slice or even via the bath. A spread of KA by diffusion in the recording chamber should be able to traverse a section in the tissue. We tested this by preparing longitudinal slices with a cut (Fig. 3B) made to separate two portions of the CA3 region, of ~ 500 – $800 \mu\text{m}$. Injection of KA on one side of the cut induced an increase in firing, while activity was not changed on the non-injected side of the cut ($n = 4$).

Cellular effects of kainic acid injection

Extracellular data showed that firing increased dramatically and then stopped close to KA injection sites, while activity at a distance increased and was then

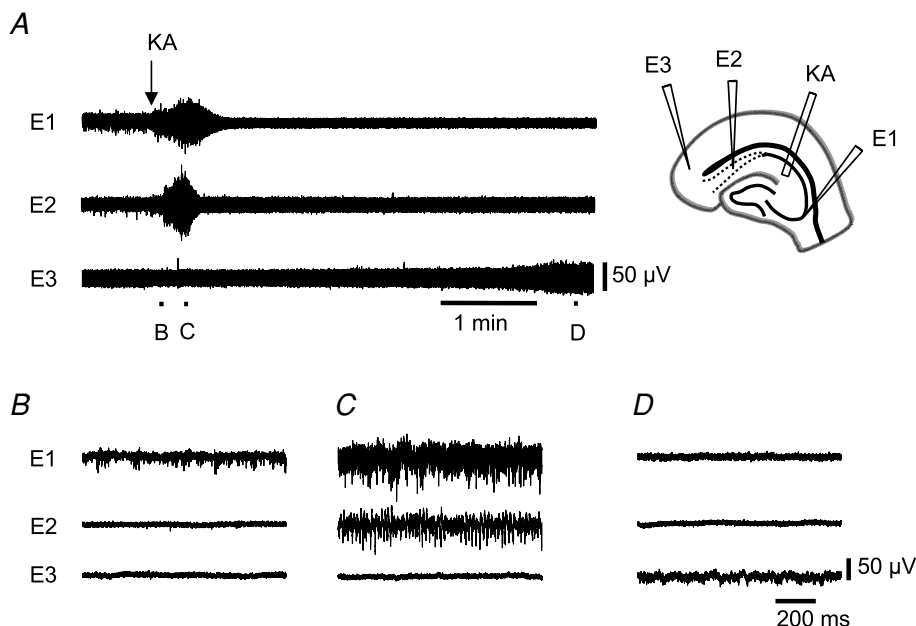


Figure 1. Response to focal KA injection in hippocampal-cortical slices

A, focal injection of kainic acid (50 nl, 20 mM) in the apical dendritic zone of the CA1 region induced an immediate increase in spontaneous activity recorded by extracellular electrodes in the CA3 area (E1) and the subiculum (E2), and a delayed increase in the entorhinal cortex (E3). B, activity before injection; C, an increase in firing with superimposed field potential oscillations recorded from the CA3 and subicular areas at 15 s after injection. D, traces taken at 5 min after KA injection show a delayed excitation in the entorhinal cortex but no activity in the CA3 region and the subiculum.

maintained. We next examined the cellular correlates of these two responses in records from close and distant sites. As shown in Fig. 4, pyramidal cells close to the injection site were strongly depolarized by KA injection ($n = 4$). The depolarization, sometimes preceded by a hyperpolarization, induced firing of duration 5–90 s at frequencies up to 200 Hz (Fig. 4A), correlated with the increase of activity in local extracellular records. After firing, all cells continued to depolarize to potentials of -40 to -10 mV, and stopped firing. The depolarization block of Na^+ -dependent action potentials was maintained. Pyramidal cell input resistance was reduced from $35 \pm 9 \text{ M}\Omega$ (mean \pm s.d., $n = 4$) before KA application, to $3 \pm 1 \text{ M}\Omega$ after injection (Fig. 4B). Hyperpolarizing current injection could not repolarize cells to potentials at which action potentials were generated.

Pyramidal cells distant from the injection site were recorded from the entorhinal cortex of hippocampal–cortical slices ($n = 3$) or at distances greater than 1.2 mm in longitudinal CA3 slices ($n = 10$). Three phases of behaviour were evident in both pyramidal cells from both types of slice, and they will be considered together (Fig. 5). During the local response to KA injection, the

membrane potential and activity of distant cells did not change. After a delay, we observed in 9 of 13 cells a membrane hyperpolarization of 3–8 mV, correlated with an increase in frequency of spontaneous IPSPs. Then pyramidal cells depolarized together with the increase in activity of local multi-unit records (Fig. 5A). Pyramidal cells were excited to potentials at which action potentials were no longer generated in 6 of 13 records at distant sites (Fig. 5B). Three of these cells repolarized, and recovered the ability to fire during records lasting up to 90 min, while the other cells remained at depolarized potentials.

Long-term actions of kainic acid in hippocampal–cortical and longitudinal CA3 slices

We observed different behaviours at sites close to and distant from KA injection during the time period of 30 min to 5 h after KA injection (Fig. 6). Close to the injection site, no extracellular unit activity was detected during this period (Fig. 6A, E1), and intracellular records could not be obtained in either hippocampal–cortical slices ($n = 9$) or longitudinal CA3 slices ($n = 22$).

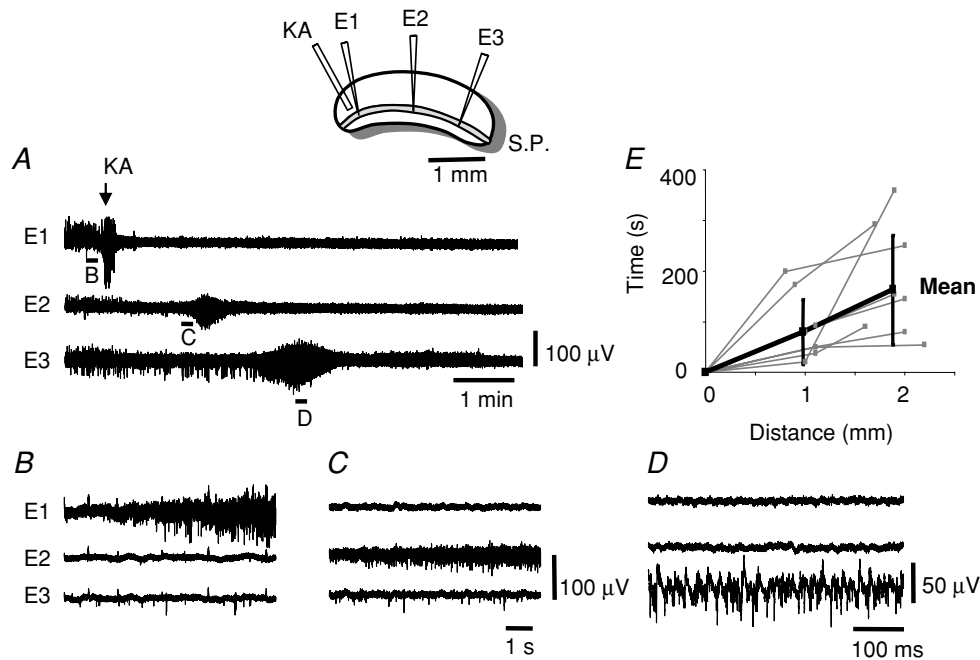


Figure 2. Response to focal KA injection in longitudinal CA3 slices

A, focal injection of kainic acid (50 nl, 20 mM) in the apical dendritic zone of the CA3 region induced an immediate increase in spontaneous extracellular activity at the site of injection, E1, and a delayed increase at distant sites, E2 and E3. Records were made from a longitudinal slice including the entire CA3 region with a separation of ~ 1 mm between E1 and E2 and between E2 and E3. B–D, details of the traces shown in A. D, field potential oscillations at 40–60 Hz are shown superimposed on the increase in firing at the distant site E3. E, the latency to the onset of the increase in firing at distant sites, measured at 10% of the maximal increase in multi-unit spike frequency, from similar experiments on nine longitudinal slices. The continuous line indicates mean latency values which provided an average propagation velocity of $9 \times 10^{-5} \pm 6 \times 10^{-5} \text{ mm ms}^{-1}$. These data suggest that the spread of firing did not slow at greater distances from the injection site.

In contrast, at distant sites in both hippocampal–cortical and CA3 longitudinal slices, multi-unit activity was often increased and sometimes rhythmic (Fig. 6A, E2). Spike frequency from the distant entorhinal cortex was typically increased in hippocampal–cortical slices. In contrast, distant sites in longitudinal CA3 slices often generated a rhythmic activity together with an oscillating field potential ($n = 10/22$ slices), with a peak power in the range 30–100 Hz (Fig. 6D). Intracellular recordings showed that interneurons discharged with most cycles of the rhythmic field potentials (Fig. 6B). Pyramidal cells

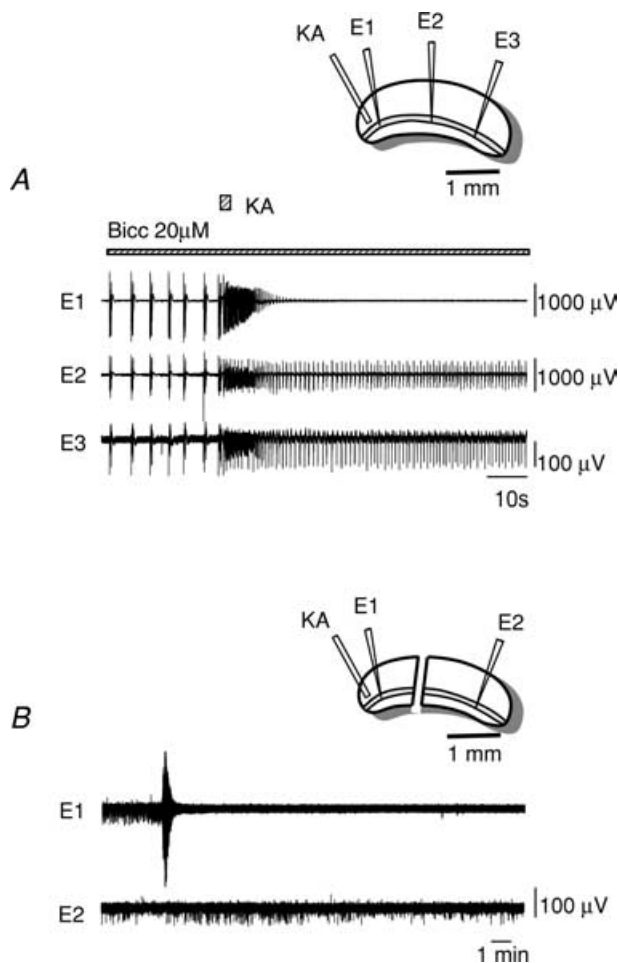


Figure 3. How does KA-induced firing spread?

A, records were made from a CA3 longitudinal slice with three electrodes, E1, E2 and E3, with each pair of electrodes separated by ~ 1 mm. Perfusion of bicuculline ($20 \mu\text{M}$) induced synchronized bursts which spread throughout the slice, a distance of ~ 2 mm. The propagation velocity was 0.12 mm ms^{-1} . Injection of kainic acid (50 nL , 20 mM) in the presence of bicuculline induced an initial increase of activity which spread with a similar speed, 0.15 mm ms^{-1} . After the initial activity induced by the KA injection, discharges near the injection site, E1, ceased, while the frequency of interictal-like activity at E2 and E3 was persistently increased. *B*, a longitudinal CA3 slice was cut into two pieces that were placed in the recording chamber with a separation of $\sim 500 \mu\text{m}$. KA injection increased firing in the injected slice, E1, but not in the separated slice, E2.

received inhibitory synaptic potentials with each cycle, and fired less frequently (Fig. 6C). These are the characteristics of gamma oscillations (Traub *et al.* 1998). Consistent with a role for GABA_A -mediated inhibition in the patterning of gamma oscillations *in vitro*, addition of the antagonist bicuculline ($20 \mu\text{M}$) suppressed the rhythmic activity, and induced interictal-like population bursts at intervals of 1–6 s ($n = 3$, not shown).

Gamma-frequency oscillations emerged with a delay of 20–30 min after KA injection. Figure 6E shows power–frequency histograms for one recording constructed at different times before, during and after the excitation induced by KA injection. The increase in the coherence of oscillations was quantified by measuring the mean power in the gamma frequency range 30–100 Hz. For 10 slices, the mean power increased from a control value of $0.07 \pm 0.04 \mu\text{V}^2$ to a peak of $2.8 \pm 3.89 \mu\text{V}^2$ during the KA-induced increase in firing. At 10–20 min after KA injection, the power was reduced to $0.13 \pm 0.12 \mu\text{V}^2$.

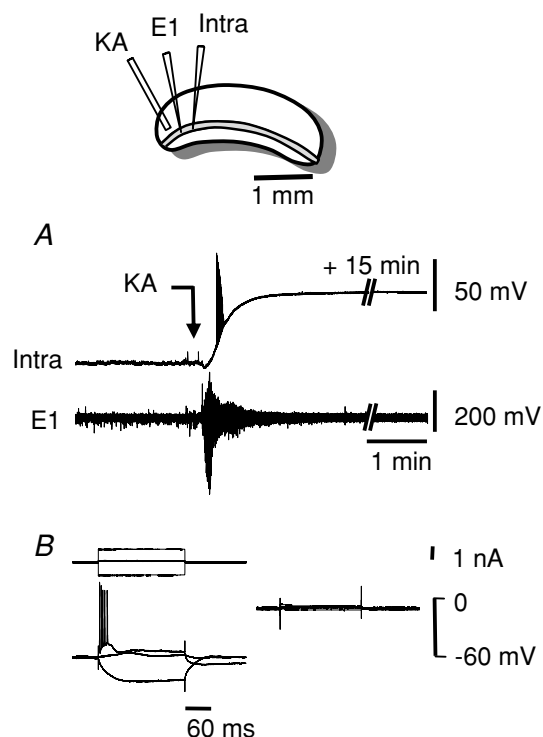


Figure 4. KA induces a depolarization block in cells close to the injection

A, intracellular (Intra) and extracellular (E1) records made in a CA3 longitudinal slice at a distance of ~ 0.3 mm from KA injection. KA induced an increase in multi-unit firing of duration about 2 min. The pyramidal cell was initially hyperpolarized by ~ 5 mV and then depolarized strongly. Firing at high frequency for ~ 15 s was succeeded by a further depolarization to about -10 mV. The depolarized membrane potential was maintained for more than 60 min. *B*, pyramidal cell responses to current injection before and after kainate application. The membrane input resistance was much reduced after KA-induced depolarization.

A considerable increase in the power of oscillations then occurred, to $5.08 \pm 6.15 \mu\text{V}^2$ at 50–70 min and $4.01 \pm 6.34 \mu\text{V}^2$ at 90–120 min after injection (Fig. 6E).

Long-term actions of kainic acid injection in *ex vivo* slices

KA injection in slices led to a maintained suppression of activity at the injection site, and an increased, often synchronous, activity at distant sites. We compared these effects with the activity generated by slices from animals injected with KA (Fig. 7). In this way, we could not only compare the effects of *in vitro* and *in vivo* KA injections, but also examine the effects of KA injection in the contralateral, non-injected hippocampus. KA was injected together with the fluorescent marker microruby so that the injection site could be identified. Up to six hippocampal–cortical slices were cut and kept in order that records could be made from ipsilateral sites close to and distant from the injection. Slices were also prepared from the hemisphere contralateral to the injection, and stored in order. Figure 7D shows a 3-D reconstruction of the spread of the tracer Rhodamine dextran (molecular mass 10 kDa) injected with kainate. At 3 h, the molecule was detected at distances of $\sim 500 \mu\text{m}$ from the injection site in the dorsal–ventral plane of the hippocampus and in the plane of the CA1 dendritic axis, with a rather larger spread of $\sim 800 \mu\text{m}$ especially towards the subiculum in the plane orthogonal to the dendritic axis and along the hippocampal fissure.

Little or no multi-unit activity was detected near the injection site in ipsilateral slices from six animals during the period 2–5 h after KA injection *in vivo* (Fig. 7A). In contrast, slices prepared from distant sites generated a robust extracellular activity (Fig. 7B). This consisted of unit discharges together with interictal-like field potentials of duration 40–120 ms, which recurred at a frequency of 0.5–3 Hz. This activity was initiated in the CA3 or CA1 regions and propagated to the dentate gyrus and the subiculum (Fig. 7B, $n = 10$ ipsilateral slices).

An interictal-like activity was also recorded at 2–5 h after KA injection in hippocampal–cortical slices from the contralateral hemisphere (Fig. 7C, $n = 15$). Figure 7E shows that population oscillations were generated only by distant ipsilateral slices, and most frequently by contralateral slices distant from the exact counterpart to the injection site. We also examined longitudinal slices prepared from the ipsi- and contralateral CA3 region of injected animals ($n = 6$). Activity was robust, and interictal-like activity was generated by three of six slices (not shown). Thus, population oscillations are generated by both ipsilateral and contralateral hippocampus at a delay corresponding to the expression of status epilepticus *in vivo*. They are generated at a distance, rather than at the injection site, and while injected slices generate

gamma oscillations, slices from injected animals generate interictal-like activity.

Effects of kainic acid injection on cell survival: Gallyas stain

We next used the Gallyas stain (Gallyas *et al.* 1980) to ask how neuronal cell death at distinct ipsilateral and contralateral sites was associated with electrical activity. Staining was done on tissue obtained from animals at 3 h after KA injection.

Near the injection site, many cells were black with silver accumulation (Fig. 8A) indicating cellular damage, in the CA1 and CA3 regions, but not the dentate gyrus. Cell death was reduced with distance. At 1.5–2 mm from the injection site, there was some loss of CA1 pyramidal cells, CA3 cells were less affected, and no cell death was evident in the dentate gyrus (Fig. 8B). There was no loss of pyramidal cells at any sections obtained from the hippocampus contralateral to KA injection (Fig. 8C; Table 1).

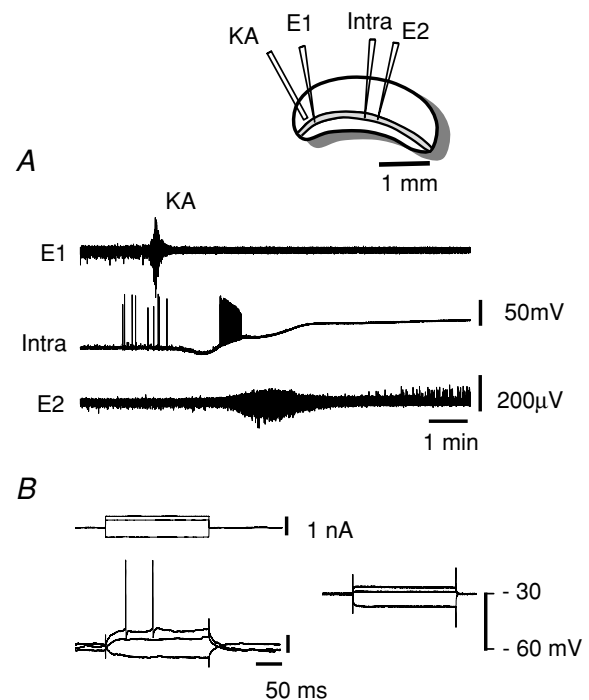


Figure 5. KA depolarizes distant cells with a delay

A, intracellular and extracellular records (E1 and E2) in a CA3 longitudinal slice. The electrode E1 was located at about 0.3 mm from KA injection, the intracellular pyramidal cell record at about 1.2 mm and the electrode E2 at 1.5 mm. KA injection induced a short latency increase in multi-unit firing at electrode E1. At electrode E2, firing increased with a latency of ~ 2 min. In the pyramidal cell, a hyperpolarization, consisting of a high-frequency barrage of IPSPs, preceded a depolarization at a latency of 1.7 min. The cell fired at high frequency for 30 s, and then depolarized in two stages to -20 mV. B, pyramidal cell responses to current injection before and after kainate application. The membrane potential of this cell remained depolarized until the end of the recording.

GABAergic inhibitory cells may be selectively vulnerable to KA (Oliva *et al.* 2002), and their loss might contribute to population oscillations in the hippocampus. We examined the survival of GABAergic cells using the Gallyas stain to identify cells with somata outside the s. pyramidale. Ipsilaterally, the degree of interneurone loss was largely correlated with that of pyramidal cells. Many degenerating interneurons were evident in all hippocampal subfields near the injection site. The number of degenerating cells was reduced with distance. In the contralateral hippocampus there was no evidence for degenerating interneurons.

A more detailed view of inhibitory cell survival (Fig. 9) was obtained by immunohistochemical studies on the

distribution of cells expressing the markers parvalbumin (PV), calbindin (CB), somatostatin (SOM) and calretinin (CR). We compared results from animals killed at 3 h. after KA injection and after injection of saline solution.

All interneurone types exhibited signs of degeneration in ipsilateral hippocampus near the site of KA injection (Bouilleret *et al.* 2000; Matyas *et al.* 2004). The numbers of PV-immunopositive cells, CB-immunoreactive interneurons and SOM-positive cells were greatly reduced (Fig. 9). CR-immunoreactive interneurons were present in the hilus but absent elsewhere (not shown). In ipsilateral hippocampus distant from the injection, interneurone damage was less than at the injection site, but still significant (not shown). The most strongly

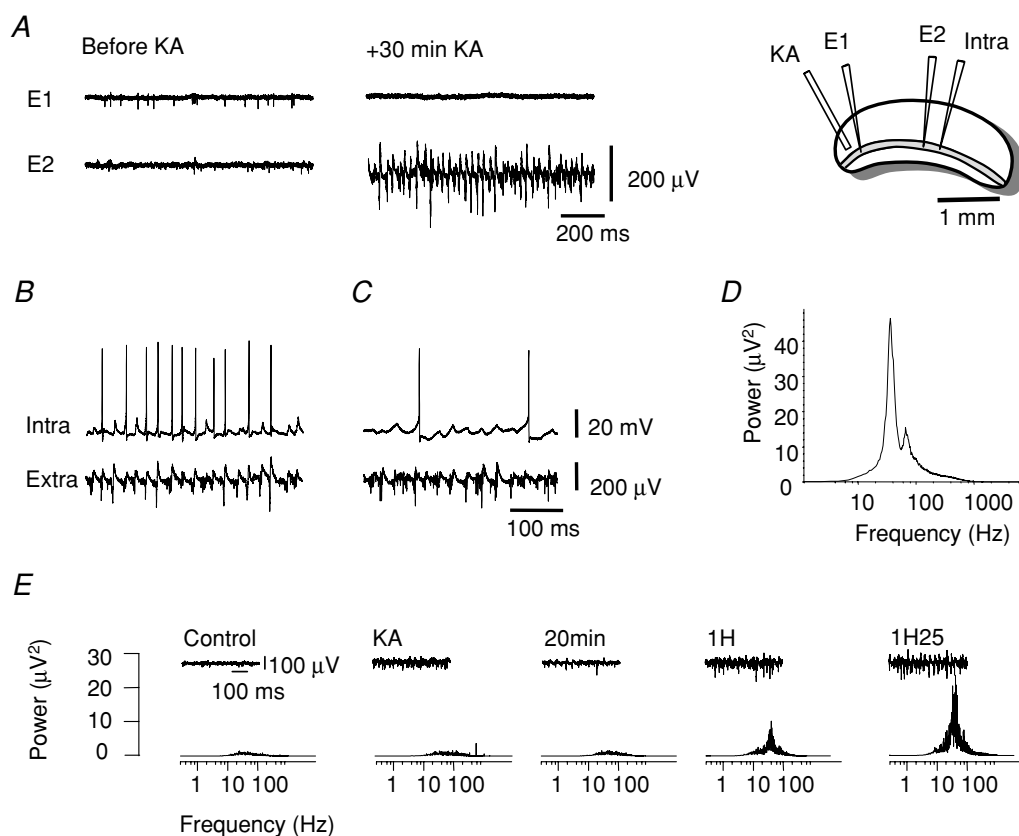


Figure 6. Delayed activity after KA injection *in vitro*

A, extracellular records, E1 close to the KA injection site, and E2 at a distance of 1.5 mm, from a longitudinal CA3 slice before and 30 min after injection. Multi-unit activity at electrode E1 was suppressed and did not recover after injection. Electrode E2 recorded large-amplitude field potentials at 30 min after kainate injection. B, recording from an inhibitory cell (near electrode E2 from A) at 30 min after kainate application. The cell either fired in phase with the local field potential or received synchronous EPSPs. C, record of a pyramidal cell (Intra) and a local field potential (Extra) from a different slice at 30 min after KA injection. Events in the local field potential record were correlated with large intracellular IPSPs. The pyramidal cell fired occasionally on recovery from an IPSP. D, power spectrum of the record from electrode E2 at 30 min in A showed a major peak at 38 Hz and a smaller peak near 80 Hz. E, changes in the power spectrum of an extracellular record with time before, during and after KA injection from a different experiment. The electrode was located at 1.2 mm from the KA injection site. KA injection induced an increase in the power with a peak near 40 Hz, but the power was reduced at 15 min after injection. A large increase in power with a peak at 40 Hz occurred between 20 and 35 min. The increase was maintained for over 90 min.

affected subgroups of interneurons were the CB-, CR- and SOM-immunoreactive cells (Fig. 9Ba and Ca), but a considerable loss of PV-immunopositive interneurons was also evident (Fig. 9Aa). Cell loss was reduced with increasing distance from the injection site. In the contralateral hippocampus, there was no loss of interneurons, even at sites strictly contralateral to the injection (Fig. 9Ab, Bb and Cb; Table 2).

Discussion

We have examined processes intervening between intrahippocampal injection of KA and the emergence

of status epilepticus in hippocampal slices and slices obtained from injected animals. Cells close to the injection site fired strongly but transiently, and then entered a long-lasting state of depolarization block. Activity induced by KA propagated slowly. The slow spread was limited by inhibitory synaptic processes, since the speed was increased when inhibition was suppressed. At distant sites, a strong initial firing was succeeded by an excitation that was maintained over several hours. The nature of the activity induced by *in vitro* and *in vivo* injections was different. In slices injected *in vitro*, rhythmic population oscillations at gamma frequencies were generated, and strengthened with time. In slices prepared from distant

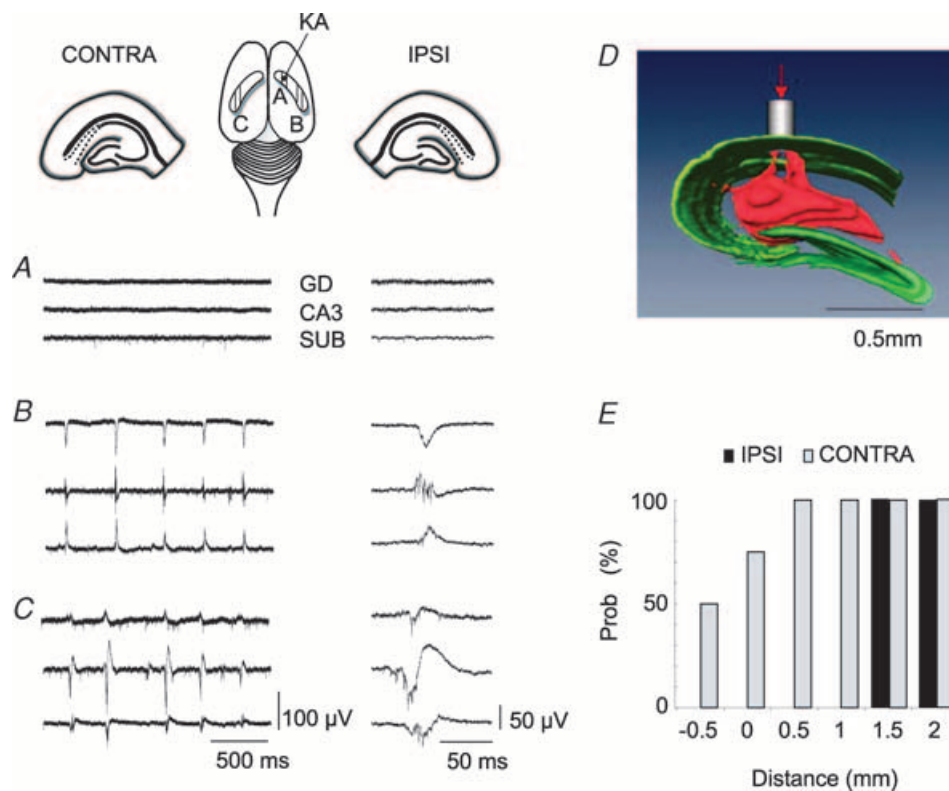


Figure 7. Delayed activity in slices prepared after KA injection *in vivo*

Hippocampal–cortical slices were prepared from the ipsilateral, KA-injected, and the contralateral hemisphere. The injection site was identified by the presence of the fluorescent marker microruby co-injected with KA, and slices were maintained in order. Extracellular records were from the dentate gyrus, GD, CA3 region, CA3, and from the subiculum, SUB, at 2–5 h after KA injection *in vivo*. A, little or no multi-unit activity was detected in slices prepared from near the injection site. Both ipsilateral slices distant from the injection site, B, and contralateral slices, C, generated a spontaneous interictal-like activity. This activity originated in the CA3 or CA1 regions and spread to the dentate and the subiculum. Traces on the left and right show records at a slow and a fast time base, respectively, from the GD, CA3 and SUB in slices prepared from the three locations, A, B and C indicated in the diagram. D, 3-D reconstruction of the diffusion of Rhodamine dextran (red) injected *in vivo*, and neuronal somata corresponding to the dentate gyrus and CA3–CA1 cell body layers (green, Neurotrace). The image was constructed from ~800 confocal images over a distance of 1.2 mm. The injection cannula entered, as indicated, from the top left. Rhodamine dextran formed a spherical cloud around the injection site with a favoured diffusion towards the subiculum probably via the hippocampal fissure. E, the probability with which interictal-like activity was detected in slices prepared from distinct ipsilateral and contralateral sites with respect to the injection. Only distant ipsilateral sites generated spontaneous oscillations. Contralateral sites that mirrored distant ipsilateral sites were more likely to generate oscillations than those that mirrored the injection site. Data for this graph were obtained from 17 ipsilateral slices and 19 slices contralateral to KA injection in four animals.

Table 1. Morphological changes in the hippocampus of KA injected mice, at 3 h after injection

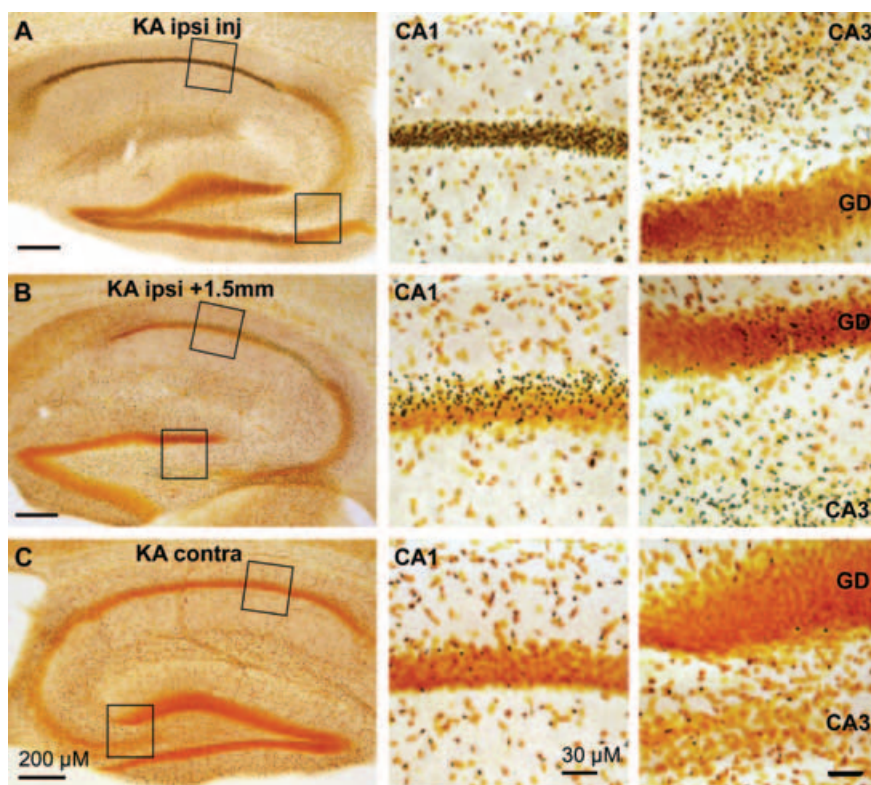
	Principal cells	PV	CB	CR	SOM
Ipsilateral, near the injection site	–	–	–	–	–
Ipsilateral, far from the injection site	++	++	+	+	+
Contralateral, near the injection site	+++	+++	+++	+++	+++
Contralateral, far from the injection site	+++	+++	+++	+++	+++

The proportion of healthy principal cells (based on Gallyas staining) and the number of surviving interneurons are shown on semiquantitative scale. +++, 90–100% of the cells are present, similar to saline-injected control; ++, slight cell loss, 50–90% of cells present; +, moderate cell loss, 10–50% of cells present; –, profound or total cell loss, 0–10% of cells present.

sites ipsilateral to KA injection *in vivo* and from the contralateral hippocampus, a rhythmic interictal-like activity was generated. Gallyas silver staining revealed a high proportion of damaged cells near the injection, but little or no cell loss in the contralateral hippocampus. Our data suggest that hippocampal population activities generated at sites distant from KA injection may contribute to status epilepticus.

Depolarization block and death of cells near the injection site?

We injected small volumes of high concentrations of KA both *in vivo* and *in vitro* in an attempt to mimic procedures used to produce status epilepticus in the intact animal (Bouilleret *et al.* 1999). Near sites of KA injection *in vitro*, multi-unit records revealed a strong but

**Figure 8. Cell degeneration following KA injection *in vivo***

Gallyas-stained tissue from animals perfused at 3 h after KA injection. Whole hippocampus and regions of the CA1, CA3 and dentate gyrus regions are shown from close to the injection site (A) and distant (B), in the ipsilateral hemisphere, and from C, the mirror to the injection site in the hemisphere contralateral to the injection. Healthy cells are coloured orange, and degenerating cells are black corresponding to precipitation of silver salts. The density of degenerating cells was very high at the injection site, and moderately high at a distance of 1.5 mm in the ipsilateral hippocampus. No degeneration was evident contralaterally.

transient firing that lasted for 2 or 3 min. No further activity was recorded for the duration of the experiment (Figs 1 and 2). This is consistent with data showing that high concentrations of KA induce neuronal necrosis (Fujikawa *et al.* 2000), although slower apoptotic mechanisms may also be initiated (Pollard *et al.* 1994). Pyramidal cells depolarized to membrane potentials where firing was no longer observed (Fig. 4). A similar fast transition to a state of depolarization block occurs in the dorsal motor vagal nucleus following ischaemia (Muller & Ballanyi, 2003), and in the hippocampus after anoxia (Dzhala *et al.* 2001) or KA application (Robinson & Deadwyler, 1981). Such depolarizations induce a

Table 2. Interneurone survival on a semiquantitative scale in the ipsilateral hippocampus of kainate-injected mice, 3 h after the injection, ~1.5 mm from the injection site

	PV	CB	CR	SOM
GD	++	–	+	+
CA3	++	–	–	–
CA1	++	+	–	+

Significance of +, ++, +++ and – as in Table 1.

maintained calcium entry (Choi, 1987) and initiate cell swelling (Nadler *et al.* 1978; Oliva *et al.* 2002) which are precursors of cell death. The cellular degeneration near the injection site observed with the Gallyas stain

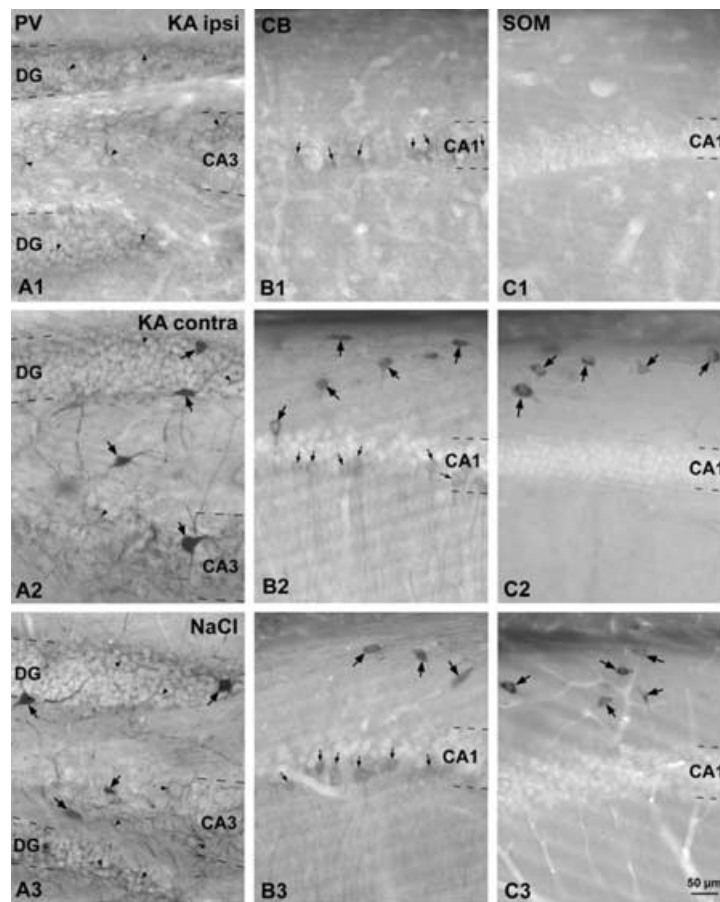


Figure 9. Interneurone changes after KA injection *in vivo*

PV-, CB- and SOM-immunostained hippocampal sections from animals perfused at 3 h after KA or NaCl injection. A1, B1 and C1 show tissue from the ipsilateral hippocampus near the injection site. A2, B2 and C2 show tissue from the non-injected hippocampus. A3, B3 and C3 show data from animals injected with NaCl. A1, A2 and A3, PV-immunopositive elements in the dentate gyrus and CA3 region. In the ipsilateral hippocampus, the number of PV-positive cells dramatically decreased, but axonal staining was visible (A1, arrowheads). The number and distribution of PV-immunoreactive elements in contralateral hippocampus (A2) was similar to the control (A3). Arrows point to somata and arrowheads show axonal elements. B1, B2 and B3, CB-immunopositive elements in the CA1 region. No CB-positive interneurons were detected near the KA injection site, but CA1 pyramidal cells were immunoreactive for CB (B1, small arrows). The distribution and number of CB-positive pyramidal cells (little arrows of Bb, Bc) and interneurons (large arrows of B2, B3) was similar in NaCl-injected animals and in the contralateral hippocampus of KA-injected animals. C1, C2 and C3, SOM-immunoreactive interneurons of the CA1 region. No SOM-positive interneurons were detected near the injection site (C1). The number and location of SOM-positive interneurons (arrows) were similar in the contralateral hippocampus of KA-injected animals (C2) and in NaCl-injected animals (C3). Scale bar for all images: 50 μ m.

(Fig. 8) confirmed that KA injection induces a local cell death.

Spread of kainate-induced excitation

The activity induced by KA injection propagated through longitudinal slices of the CA3 region at a velocity close to $1 \times 10^{-4} \text{ mm ms}^{-1}$ (Fig. 2). This is much slower than the spread of synchronous discharges initiated by disinhibition, 0.12 mm ms^{-1} (Miles *et al.* 1988). Disinhibition-induced synchrony in the CA3 region spreads by a polysynaptic process in which cell firing synaptically excites distant cells, which then excite still more distant cells. In contrast, intracellular records revealed that a travelling wavefront of inhibitory synaptic events preceded the KA-induced excitation in pyramidal cells (Figs 4 and 5). Since KA-induced firing spread more quickly in the presence of bicuculline (Fig. 3A), we conclude that synaptic inhibition normally prevents the propagation of KA-induced firing by polysynaptic pathways.

If the activity initiated by KA does not spread synaptically, how does it spread? KA might simply diffuse throughout the slice inducing firing as it spreads. Using reasonable values for the diffusion coefficient of KA ($4 \times 10^{-6} \text{ cm}^2 \text{ s}^{-1}$), tortuosity (1.65) and extracellular volume fraction (0.15), the diffusion equation (Nicholson, 2001) suggests that at a distance of 2 mm, the peak concentration of KA should be reached after a delay of 30–50 min. Lower concentrations that may increase cell firing will arrive more quickly. However, neuronal firing induced by KA will also initiate local processes that facilitate propagation, including an increase in extracellular K^+ and the liberation of glutamate. These processes should recruit cells to the excited ensemble, and accelerate the spread of firing. The spread of neuronal excitation induced by KA injection might then resemble a spreading depression (Lauritzen *et al.* 1988). Indeed, spreading depression in hippocampus propagates at speeds close to $10^{-4} \text{ mm ms}^{-1}$ (Snow *et al.* 1983; Herreras *et al.* 1994; Peters *et al.* 2003), similar to those we measured.

A delayed emergence of 40–60 Hz synchrony at distant sites *in vitro*

KA induced high-frequency firing and oscillating field potentials in the gamma frequency range both in response to injection and with a delay at distant sites in CA3 slices. During these oscillations (Fig. 6B and C), interneurone firing was phase-locked to the local field potential, while pyramidal cells fired infrequently and received a rhythmic inhibition (Whittington *et al.* 1995; Fisahn *et al.* 1998).

The power of gamma frequency oscillations increased significantly, with a delay of several tens of minutes after KA injection (Fig. 6E). Maybe the power of oscillations is enhanced by the reconfiguration of neuronal circuits

dependent on the loss of pyramidal cells and some types of interneurons, although we note the peri-somatic parvalbumin-positive cells were largely spared (Table 2). If KA induces a wave of activity that propagates by mechanisms similar to a spreading depression, but faster than diffusion, then a second wave of KA diffusion might underlie the delayed emergence of gamma oscillations. Alternatively, gamma frequency activity may itself initiate self-reinforcing synaptic (Whittington *et al.* 1997; Lauri *et al.* 2003), cellular (Melyan *et al.* 2002), or even axonal (Semyanov & Kullmann, 2001) plasticity. The present data do not let us discriminate between these different sites for changes that might underlie the delayed enhancement of gamma oscillations (Ben-Ari & Gho, 1988; Khalilov *et al.* 1999; Khalilov *et al.* 2003).

Differences between delayed activity in injected slices and slices from injected animals

At sites near *in vitro* KA injections, or in slices close to *in vivo* injection sites, we observed no neuronal activity after 2–5 h. The two approaches both revealed an enhanced, often rhythmic, activity at distant sites. However the nature of the activity was not the same. Gamma-frequency oscillations were observed at 2–5 h at distant sites in injected slices, whereas slices prepared from injected animals generated an interictal-like activity (Fig. 7). Previous work reveals a similar difference which remains unexplained. In slices for instance, bath application of similar concentrations of KA has been shown to induce either interictal-like (Westbrook & Lothman, 1983; Fisher & Alger, 1984) or gamma-frequency activity (Vreugdenhil *et al.* 2003; Fisahn *et al.* 2004).

The reason for this difference is not clear. Similar concentrations and volumes of KA were injected in the same way from the same catheter system in both slices and animals. Possibly gamma oscillations may be transformed with time into an interictal-like activity. Gamma oscillations were generated in injected slices at latencies between 20 min and 3 h 30 min after injection. Both ipsilateral and contralateral slices from injected animals generated interictal-like activity at latencies of 2–5 h after injection. One difference might be the circuits involved. Gamma activity was generated at distant CA3 sites after KA injection in longitudinal CA3 slices, but not at distant entorhinal sites after injections into combined hippocampal–cortical slices. Even so, interictal rather than gamma oscillations were observed in longitudinal CA3 slices prepared from injected animals. Another difference might be the injection site. In longitudinal slices, injections were made at apical dendritic sites of the CA3 region, while KA was injected *in vivo* in CA1 dendritic regions. Possibly, the distinct neuronal elements activated by injection at these different sites influence the nature of the delayed

population activity. Finally, injection in the intact animal probably activates distant structures that may initiate distinct modulating influences absent in a slice. In order to affect hippocampal activity, such influences should operate in long-range recurrent fashion.

Relations between status epilepticus and kainate-induced activity *in vitro*

Is the delayed rhythmicity observed *in vitro* related to the behavioural manifestations of status epilepticus? While our data show that the injected site cannot contribute, delayed activity generated at distant sites in the injected and also in the contralateral hippocampus is probably involved. Clearly, activities of non-hippocampal structures are likely to be involved.

Both the injected and the contralateral hippocampus independently generated delayed interictal activity (Fig. 7B and C). A comparison may illuminate the nature of the effective stimulus needed to initiate this activity. It seems unlikely that injected KA penetrated to the contralateral hippocampus. Furthermore we could not detect a cell loss in the non-injected hippocampus (Fig. 8). Thus, population oscillations in the contralateral hippocampus probably depend on changes induced by activity in the injected hippocampus. Such changes have been described in a preparation comprising both hippocampi from young animals, and ascribed to activity-dependent changes in the reversal potential for GABAergic signalling (Khalilov *et al.* 2003). However it is difficult to interpret our data within the framework of a mirror focus. First, we showed that the duration of high-frequency firing at the injection site was less than 3 min. Secondly, the probability that contralateral slices that strictly mirrored the injection site generated delayed oscillations was less than that for slices contralateral to sites distant from KA injection (Fig. 7E). Thirdly, our data suggest that the spread of KA-induced activity by axonal propagation and synaptic transmission is suppressed by synaptic inhibition (Fig. 3A). We note that in young animals GABAergic signalling should be depolarizing, thus favouring an axonal and synaptic spread. One way to reconcile these constraints is to suggest that contralateral interictal activity is not induced by the immediate transient firing near the injection site, but rather results from activity-dependent mechanisms initiated by the delayed population oscillations generated at ipsilateral sites distant to KA injection. This hypothesis could be tested by comparing the time course with which interictal activities develop at distant ipsilateral sites and in the contralateral hippocampus *in vivo*.

Similar epileptic activity with different morphology

Both distant ipsilateral hippocampus and contralateral hippocampus generate a delayed interictal-like activity

(Fig. 8). Patterns of cell survival at the time that the activity was generated were considerably different. There was a moderate cell loss of both CA1 and CA3 pyramidal cells, and also interneurons in all regions at distant sites ipsilateral to the injection site. In contrast, no loss of principal cells or interneurons was detected in contralateral hippocampus (Fig. 9). This suggests that morphologically different neuronal networks can generate similar population activities, and also that cell death is not a necessary factor for the generation of epileptiform activity in the hippocampus.

References

- Baram TZ, Gerth A & Schultz L (1997). Febrile seizures: an appropriate-aged model suitable for long-term studies. *Dev Brain Res* **98**, 265–270.
- Ben-Ari Y (1985). Limbic seizure and brain damage produced by kainic acid: mechanisms and relevance to human temporal lobe epilepsy. *Neuroscience* **14**, 375–403.
- Ben-Ari Y & Cossart R (2000). Kainate, a double agent that generates seizures: two decades of progress. *Trends Neurosci* **23**, 580–587.
- Ben-Ari Y & Gho M (1988). Long-lasting modification of the synaptic properties of rat CA3 hippocampal neurones induced by kainic acid. *J Physiol* **404**, 365–384.
- Ben-Ari Y, Lagowska J, Tremblay E & Le Gal La Salle G (1979). A new model of focal status epilepticus: intra-amygdaloid application of kainic acid elicits repetitive secondarily generalized convulsive seizures. *Brain Res* **63**, 176–179.
- Bouillere V, Loup F, Kiener T, Marescaux C & Fritschy JM (2000). Early loss of interneurons and delayed subunit-specific changes in GABA(A)-receptor expression in a mouse model of mesial temporal lobe epilepsy. *Hippocampus* **10**, 305–324.
- Bouillere V, Ridoux V, Depaulis A, Marescaux C, Nehlig A & Le Gal La Salle G (1999). Recurrent seizures and hippocampal sclerosis following intrahippocampal kainate injection in adult mice: electroencephalography, histopathology and synaptic reorganization similar to mesial temporal lobe epilepsy. *Neuroscience* **89**, 717–729.
- Chen K, Aradi I, Thon N, Eghbal-Ahmadi M, Baram TZ & Soltesz I (2001). Persistently modified h-channels after complex febrile seizures convert the seizure-induced enhancement of inhibition to hyperexcitability. *Nat Med* **7**, 331–337.
- Choi DW (1987). Ionic dependence of glutamate neurotoxicity. *J Neurosci* **7**, 369–379.
- Cohen & Miles (2000). Contributions of intrinsic and synaptic activities to the generation of neuronal discharges *in vitro* hippocampus. *J Physiol* **524**, 485–502.
- Cossart R, Dinocourt C, Hirsch JC, Merchán-Pérez A, De Felipe J, Ben-Ari Y, Esclapez M & Bernard C (2001). Dendritic but not somatic GABAergic inhibition is decreased in experimental epilepsy. *Nat Neurosci* **4**, 52–62.
- Dzhala V, Khalilov I, Ben-Ari Y & Khazipov R (2001). Neuronal mechanisms of the anoxia-induced network oscillations in the rat hippocampus *in vitro*. *J Physiol* **536**, 521–531.

- Fisahn A, Contractor A, Traub RD, Buhl EH, Heinemann SF & McBain CJ (2004). Distinct roles for the kainate receptor subunits GluR5 and GluR6 in kainate-induced hippocampal gamma oscillations. *J Neurosci* **24**, 9658–9668.
- Fisahn A, Pike FG, Buhl EH & Paulsen O (1998). Cholinergic induction of network oscillations at 40 Hz in the hippocampus in vitro. *Nature* **394**, 186–189.
- Fisher RS & Alger BE (1984). Electrophysiological mechanisms of kainic acid-induced epileptiform activity in the rat hippocampal slice. *J Neurosci* **4**, 312–323.
- Fujikawa DG, Shinmei SS & Cai B (2000). Kainic acid-induced seizures produce necrotic, not apoptotic, neurons with internucleosomal DNA cleavage: implications for programmed cell death mechanisms. *Neuroscience* **98**, 41–53.
- Gallyas F, Zaborszky L & Wolff JR (1980). Experimental studies of mechanisms involved in methods demonstrating axonal and terminal degeneration. *Stain Technol* **55**, 281–290.
- Goddard GV (1967). Development of epileptic seizures through brain stimulation at low intensity. *Nature* **214**, 1020–1021.
- Herreras O, Largo C, Ibarz JM, Somjen GG & Martin del Rio R (1994). Role of neuronal synchronizing mechanisms in the propagation of spreading depression in the in vivo hippocampus. *J Neurosci* **14**, 7087–7098.
- Jensen FE, Applegate CD, Holtzman D, Belin TR & Burchfiel JL (1991). Epileptogenic effect of hypoxia in the immature rodent brain. *Ann Neurol* **29**, 629–637.
- Khalilov I, Dzhala V, Medina I, Leinekugel X, Melyan Z, Lamsa K, Khazipov R & Ben-Ari Y (1999). Maturation of kainate-induced epileptiform activities in interconnected intact neonatal limbic structures in vitro. *Eur J Neurosci* **11**, 3468–3480.
- Khalilov I, Holmes GL & Ben-Ari Y (2003). In vitro formation of a secondary epileptogenic mirror focus by interhippocampal propagation of seizures. *Nat Neurosci* **6**, 1079–1085.
- Lauri SE, Bortolotto ZA, Nistico R, Bleakman D, Ornstein PL, Lodge D, Isaac JT & Collingridge GL (2003). A role for Ca²⁺ stores in kainate receptor-dependent synaptic facilitation and LTP at mossy fiber synapses in the hippocampus. *Neuron* **39**, 327–341.
- Lauritzen M, Rice ME, Okada Y & Nicholson C (1988). Quisqualate, kainate and NMDA can initiate spreading depression in the turtle cerebellum. *Brain Res* **475**, 317–327.
- Magloczky Z & Freund TF (1993). Selective neuronal death in the contralateral hippocampus following unilateral kainate injections into the CA3 subfield. *Neuroscience* **56**, 317–335.
- Matyas F, Freund TF & Gulyas AI (2004). Immunocytochemically defined interneuron populations in the hippocampus of mouse strains used in transgenic technology. *Hippocampus* **14**, 460–481.
- Melyan Z, Wheal HV & Lancaster B (2002). Metabotropic-mediated kainate receptor regulation of IsAHP and excitability in pyramidal cells. *Neuron* **34**, 107–114.
- Miles R, Traub RD & Wong RKS (1988). Spread of synchronous firing in longitudinal slices from the CA3 region of the hippocampus. *J Neurophysiol* **60**, 1481–1496.
- Misonou H, Mohapatra DP, Park EW, Leung V, Zhen D, Misonou K, Anderson AE & Trimmer JS (2004). Regulation of ion channel localization and phosphorylation by neuronal activity. *Nat Neurosci* **7**, 711–718.
- Muller M & Ballanyi K (2003). Dynamic recording of cell death in the in vitro dorsal vagal nucleus of rats in response to metabolic arrest. *J Neurophysiol* **89**, 551–561.
- Nadler JV, Perry BW & Cotman CW (1978). Intraventricular kainic acid preferentially destroys hippocampal pyramidal cells. *Nature* **271**, 676–677.
- Nicholson C (2001). Diffusion and related transport mechanisms in brain tissue. *Reports Prog Physics* **64**, 815–884.
- Nusser Z, Hajos N, Somogyi P & Mody I (1988). Increased number of synaptic GABA(A) receptors underlies potentiation at hippocampal inhibitory synapses. *Nature* **395**, 172–177.
- Oliva AA Jr, Lam TT & Swann JW (2002). Distally directed dendrotoxicity induced by kainic Acid in hippocampal interneurons of green fluorescent protein-expressing transgenic mice. *J Neurosci* **22**, 8052–8062.
- Peters O, Schipke CG, Hashimoto Y & Kettenmann H (2003). Different mechanisms promote astrocyte Ca²⁺ waves and spreading depression in the mouse neocortex. *J Neurosci* **23**, 9888–9896.
- Pollard H, Charriaut-Marlangue C, Cantagrel S, Represa A, Robain O, Moreau J & Ben-Ari Y (1994). Kainate-induced apoptotic cell death in hippocampal neurons. *Neuroscience* **63**, 7–18.
- Raastad M & Shepherd GMG (2003). Single-axon action potentials in the rat hippocampal cortex. *J Physiol* **548**, 745–752.
- Ribak CE, Harris AB, Vaughn JE & Roberts E (1979). Inhibitory, GABAergic nerve terminals decrease at sites of focal epilepsy. *Science* **205**, 211–214.
- Riban V, Bouillere V, Pham-Le BT, Fritschy JM, Marescaux C & Depaulis A (2002). Evolution of hippocampal epileptic activity during the development of hippocampal sclerosis in a mouse model of temporal lobe epilepsy. *Neuroscience* **112**, 101–111.
- Robinson JH & Deadwyler SA (1981). Kainic acid produces depolarization of CA3 pyramidal cells in the vitro hippocampal slice. *Brain Res* **221**, 17–27.
- Sater RA & Nadler JV (1988). On the relation between seizures and brain lesions after intracerebroventricular kainic acid. *Neurosci Lett* **84**, 73–78.
- Semyanov A & Kullmann DM (2001). Kainate receptor-dependent axonal depolarization and action potential initiation in interneurons. *Nature Neurosci* **4**, 718–723.
- Snow RW, Taylor CP & Dudek FE (1983). Electrophysiological and optical changes in slices of rat hippocampus during spreading depression. *J Neurophysiol* **50**, 561–572.
- Sutula T, He XX, Cavazos J & Scott G (1988). Synaptic reorganization in the hippocampus induced by abnormal functional activity. *Science* **239**, 1147–1150.
- Suzuki F, Hirai H, Onteniente B, Riban V, Matsuda M & Kurokawa K (2000). Long-term increase of GluR2 alpha-amino-3-hydroxy-5-methylisoxazole-4-propionate receptor subunit in the dispersed dentate gyrus after intrahippocampal kainate injection in the mouse. *Neuroscience* **101**, 41–50.

- Traub RD, Spruston N, Soltesz I, Konnerth A, Whittington MA & Jefferys GR (1998). Gamma-frequency oscillations: a neuronal population phenomenon, regulated by synaptic and intrinsic cellular processes, and inducing synaptic plasticity. *Prog Neurobiol* **55**, 563–575.
- Vreugdenhil M, Faas GC & Wadman WJ (1998). Sodium currents in isolated rat CA1 neurons after kindling epileptogenesis. *Neuroscience* **86**, 99–107.
- Walther H, Lambert JD, Jones RS, Heinemann U & Hamon B (1986). Epileptiform activity in combined slices of the hippocampus, subiculum and entorhinal cortex during perfusion with low magnesium medium. *Neurosci Lett* **69**, 156–161.
- Westbrook GL & Lothman EW (1983). Cellular and synaptic basis of kainic acid-induced hippocampal epileptiform activity. *Brain Res* **273**, 97–109.
- Whittington MA, Traub RD, Faulkner HJ, Stanford IM & Jefferys JGR (1997). Recurrent excitatory postsynaptic potential induced by synchronized fast cortical oscillations. *Proc Natl Acad Sci U S A* **94**, 12198–12203.
- Whittington MA, Traub RD & Jefferys JG (1995). Synchronized oscillations in interneuron networks driven by metabotropic glutamate receptor activation. *Nature* **373**, 612–615.
- Zaczek R & Coyle JT (1982). Excitatory amino acid analogues: neurotoxicity and seizures. *Neuropharmacology* **21**, 5–26.

Acknowledgements

We would like to thank Viviane Bouilleret and Antoine depaulis for technical help and advice with the preparation of kainate-injected animals, and Emmanuel Eugene for help with the imagery. We thank Viviane Bouilleret and Katalin Toth for their comments on the manuscript. INSERM, the NIH (MH054671), the Fondation Francaise pour la Recherche sur l'Epilepsie, the European Commission (contract 503221) and an ACI from the French Ministère de la Recherche provided financial support.